

# **In-situ X-ray microtomography tensile tests in ductile open-cell nickel foams**

**T. Dillard, F. N'Guyen, S. Forest, Y. Bienvenu, J.-D. Bartout**  
Centre des Matériaux P.M. Fourt, Ecole des Mines de Paris, France

**L. Salvo, R. Dendievel**  
GPM2, INP Grenoble, France

**E. Maire**  
GEMPPM, INSA Lyon, France

**P. Cloetens**  
European Synchrotron Radiation Facility, Grenoble, France

**C. Lantuéjoul**  
Centre de Géostatistique, Ecole des Mines de Paris, France

The aim of this paper is to describe the initial cell morphology of an open-cell nickel foam, and to follow its evolution during tension. For that purpose, in-situ X-ray microtomography tensile tests have been performed at E.S.R.F. with a resolution of 10  $\mu\text{m}$ . The first step of the 3D quantitative image analysis of the 3D reconstruction images is to close the cells in order to identify them individually. The 3D segmentation methodology is explained in detail. Then, the main parameters such as cell size distribution and the cell orientation are determined at each stage of deformation and linked to the macroscopic mechanical behaviour of nickel foams.

## **1 Introduction**

Nickel foams are used for energy storage in batteries and produced in the form of sheets or coils by the firm NiTECH. In this work, the coiling direction is called RD. The transverse and normal direction are respectively denoted TD and ND. The relative density of studied foams is 0.035. The tensile curves exhibit a non-linear elastoplastic regime followed by a regime with an almost linear hardening (see Fig.1). Badiche et al. [1] found that the response is strongly anisotropic. They relate the observed anisotropy to the aspect ratio  $R$  defined by Gibson and Ashby in their idealized anisotropic unit cell [2]. The found anisotropy  $R=1.5$  results from the preferential orientations of the starting polyurethane foam and also from the plane strain tension along RD during the manufacturing process. To quantify both contributions, a 3D study of the microstructure of foams is necessary. Indeed, cells orientation, cells shape and struts length can not be determined precisely by a 2D analysis. Moreover, recent observation using X-ray microtomography at an intermediate resolution [3] proves that this technique is suitable for the investigation of the microstructure of foams. By adding a tensile/compression machine to the experimental set-up, the evolution of the microstructure under load can be observed [4]. Thus, relationship between microstructure and properties can be established.

## **2 Experimental methods**

In-situ tensile tests using X-ray microtomography have been performed at the E.S.R.F. (Grenoble) for its high photon flux. The energy is set at 30 keV. To characterize the global behaviour of foams, a 10  $\mu\text{m}$  resolution is chosen. Accordingly, the whole gauge length

must be contained in a 10 mm diameter circle for a correct 3D reconstruction of the images. The size of the specimens with a dogbone shape is 15 mm high, 5 mm wide and 1.68 mm thick. Two scans are necessary to follow the whole area of interest during loading. Nickel foams specimens are cut by edm wire cutting and glued between plates. These plates are gripped on a tensile stage.

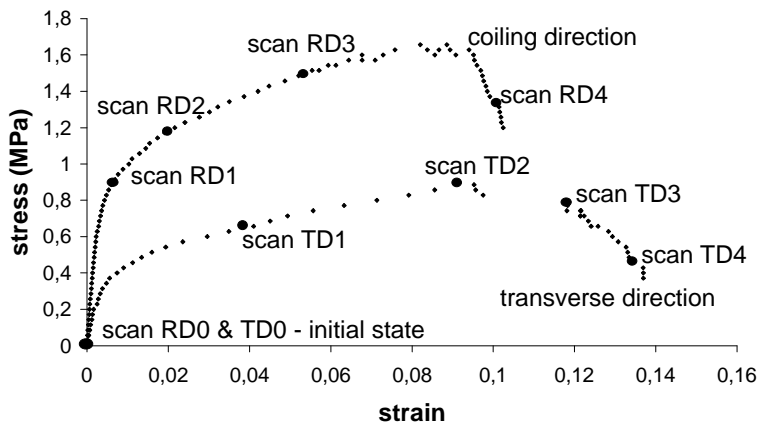
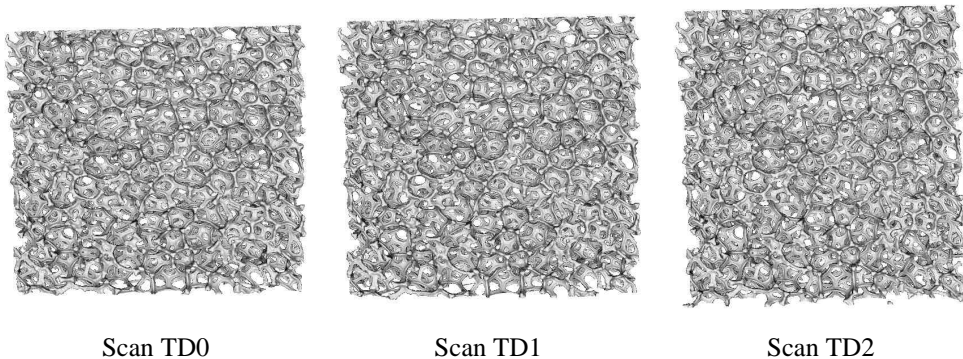


**Fig. 1.** In-situ tensile curves of the two open-cell nickel foam specimens investigated in this work

After placing the stage under the beam, a first scan consisting in 900 projections is acquired. The tensile test then begins and is interrupted for scanning the current state of the foam. Two tensile tests are carried out, the first one along direction RD and the second one along direction TD. For each test, 5 scans are performed. The positions of the scans are indicated as large black spots on the tensile curves of Fig.1. Then, the 3D rendering of the scans is computed. Fig.2 shows the 3D images reconstruction for the scans acquired during loading in the transverse direction. Crack initiates first in the top left side of the specimen. Two cracks are visible in the scan TD3 (see Fig.2). Indeed, several cracks can occur at the same time. Propagation of these cracks can also be observed in the scan TD4.



Scan TD0

Scan TD1

Scan TD2

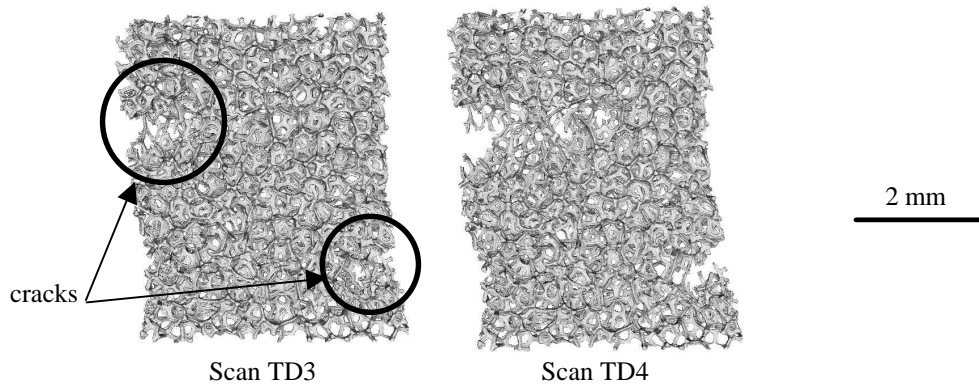


**Fig. 2.** 3D rendering of the TD scans – loading in the transverse direction TD

### 3 3D segmentation methodology

3D segmentation of the cells is necessary to characterize completely their shape. Indeed, a 3D granulometry model by openings can only reach the size of the cells. In this paper, the cells are automatically segmented by using the watershed transform of the marker distance function [5]. First, the distance map image of the cells [6] is computed (see Fig.3). Each gray tone slices of the volume, is interpreted as a topographic surface. The lighter the gray tone of a voxel is, the higher its topographic altitude is.

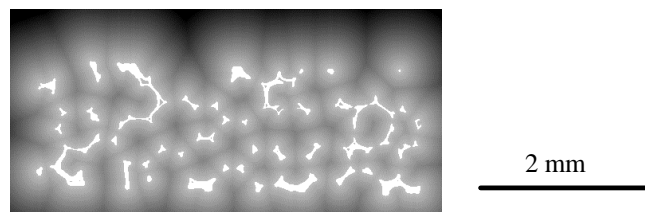


**Fig. 3.** Distance map of a 2D slice (sample loaded in the TD)

Markers, defined as the minima of the topographic volume, are represented by white spots in Fig.4a. They correspond to the ultimate eroded sets [7]. In Fig.3, 4, and 5, this algorithm is applied to a 2D section. As a result, all the markers appear in the 2D section. One and only one marker is needed for each cell. However, this basic procedure yields a severe oversegmentation (see Fig.4b). Too many markers are obtained in Fig.4a : several markers are inside the same cell, others are between two cells. To select correctly these markers, a topographic condition on the marker's neighbourhood is added. The grey level distribution around a right marker must have, due to the cell convexity, a narrow peak shape. So, 3D segmentation of open-cell foam does not only depend on the marker distance function but also, on the neighboring markers. The result of this markers'

selection is shown in the Fig.5a. Then, the reconstruction from the markers is processed by the distance function to obtain the watershed (see Fig.5b). It can be noticed that the algorithm proposed in this work seems to be more robust than Bouchet's algorithm [8]. Indeed, there is no morphological operation on the markers to select them. In brief, problem of oversegmentation is solved by using topographic considerations and all the cells are automatically closed in 3D.

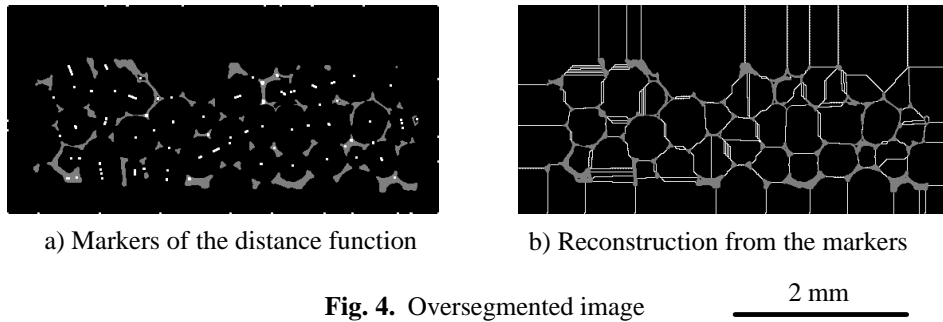


Fig. 4. Oversegmented image

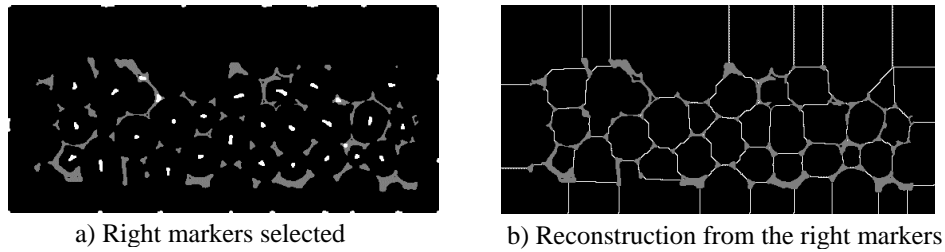


Fig. 5. Keeping the right markers by using topographic considerations

#### 4 3D quantitative analysis

A quantitative 3D analysis of the morphology of open-cell foams is carried out. The evolution of the mean geometrical parameters of the cells during straining is investigated via a volume of  $5 \times 1.6 \times 4 \text{ mm}^3$  in the RD and  $4 \times 2 \times 2 \text{ mm}^3$  in the TD (volume included between the 2 cracks of Fig.2). For that purpose, the 3D inertia matrix of the equivalent ellipsoid is determined for each cell. The 3 principal axes of the ellipsoid are denoted by  $a < b < c$ . The mean values over 130 cells in the RD and 73 cells in the TD are given in table 1. Only the results concerning the scan RD0 to RD3 and TD0 to TD2 are given in this paper because the cracks modify the shape parameters.

According to table 1, the 3 axes  $a, b, c$ , are different. After 5% loading in direction RD,  $b$  (resp.  $c$ ) is increased by 2.7% (resp. 0.5%),  $a$  is reduced by 4%. The volume variation is thus negligible. Similarly, after 9% loading in direction TD,  $a$  is increased by 10.1%,  $b$  and  $c$  are reduced by 1.3% and 2.8% respectively. It results that the volume of the foam

increases during loading in TD. Moreover, according to the shape of the cells, deformation of the cell in the TD is easier.

	Scan number	a ( $\mu\text{m}$ )	b ( $\mu\text{m}$ )	c ( $\mu\text{m}$ )	R=b/a
RD	0	404 +/- 12	511 +/- 14	624 +/-17	1,28 +/- 0.07
	1	404 +/- 12	513 +/- 14	621 +/- 16	1,28 +/- 0.07
	2	401 +/- 12	525 +/- 14	627 +/- 16	1,32 +/- 0.07
	3	388 +/-13	521 +/- 17	627 +/- 20	1,36 +/- 0.09
TD	0	406 +/- 15	521 +/- 20	611 +/- 21	1,29 +/- 0.1
	1	428 +/- 16	521 +/- 19	607 +/- 20	1,22 +/- 0.09
	2	447 +/- 18	514 +/- 18	594 +/- 19	1,16 +/- 0.09

**Table 1.** Ellipsoid mean parameters

Then, the eigen vectors of the large axis  $c$  is studied for each cell in order to know its orientation in the reference (RD,TD,ND). Figure 6 shows the stereographic projection of the large axis  $c$  in the plane (TD,RD) for the initial state and the two states (RD3 and TD2) before cracking. At the initial state (scan RD0), the axis  $c$  is almost aligned with direction ND and slightly tilted in direction RD. It shows that the effect of gravity during the foaming process of the precursor polyurethane foam is the most important for the final open-cell nickel foam structure. The tilt, induced by nickel foam processing (tension along direction RD) is of secondary importance. During traction, the large axis  $c$  of the cells moves towards the direction of loading. At the beginning, the  $c$ -projection is centered around ND (scan RD0) even though it is distributed along the axis RD in the scan RD3. The same result is found for tension along TD. However, during TD loading, the length of the smallest axis is increased. The cells become more and more spherical. The  $c$ -projection is well-distributed in the plane (RD,TD). The texture of the  $c$  axis after 8% of macroscopic deformation appears random (scan TD2). Foam structure has become more isotropic. The orientation of the  $b$  parameter has the same behaviour as  $c$  (aligned with RD during tension along RD and well-distributed in the plane (RD,TD) during tension along TD) whereas the  $a$  parameter remains aligned with TD.

The geometry aspect ratio  $R$  between the RD and TD can be determined :  $R=b/a=1.28$ . This value is not too far from the macroscopic estimation given in [1]. This difference comes from the choice of the idealized anisotropic unit cell [2]. Indeed, the Gibson and Ashby's model is computed for an unit cell with  $a=c < b$ , which is not representative of the ellipsoid parameters determined in this work, where  $a < b < c$ .

## 5 Conclusion

Open-cell nickel foams have been imaged at different stages of deformation during in-situ tensile tests at ESRF. Based on a robust 3D segmentation method, quantitative measurements on cell morphology have been performed. Results have been studied by overall statistics. Differences between eigen values of each cell at different stages have to

be analysed cell by cell to investigate possible strain heterogeneities. Moreover, with the 3D cells segmentation, the skeleton of open-cell nickel foam is available [9] and a finite element analysis on the real structure can be performed.

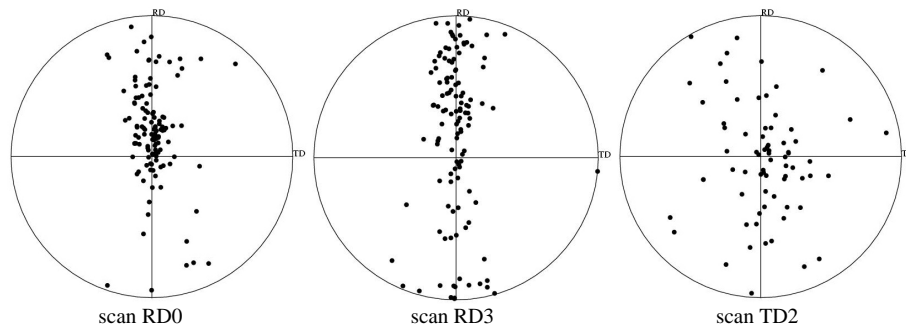


**Fig. 6.** Large axis c orientation – plane (TD,RD)

### Acknowledgements

The three first authors thank M. Croset for supplying material and stimulating discussions, the French Ministry for Industry under contract MONICKE, and finally the ID19 beam line team at E.S.R.F..

### References

- [1] X. Badiche, S. Forest, T. Guibert, Y. Bienvenu, P. Ienny, M. Croset, *Materials Science and Engineering A289*, p. 276-288 (2000)
- [2] L.J. Gibson, M.F. Ashby, “Cellular Solids, structure and properties”, Cambridge Univ. Press, 2nd Edition (1997)
- [3] A. Elmoutaouakkil, L. Salvo, E. Maire, G. Peix, *Proc. Int. Conf. Metal Foams and Porous Metal Structures*, Eds: J. Banhart, M.F. Ashby, N. Fleck (MIT-Publishing, Bremen 2001), p. 245-250
- [4] E. Maire, J.Y. Buffière, L. Salvo, J.J. Blandin, W. Ludwig, J.M. Létang, *Advanced Engineering Materials* 3, n°8, p. 539-546 (2001)
- [5] F. Meyer, S. Beucher, *Journal of Visual Communication and Image representation* 1, n°1, p.21-46 (1990)
- [6] J. Serra, “Image Analysis and Mathematical morphology, Volume 2 : Theoretical advances”, Academic Press, 1988
- [7] C. Lantuéjoul, F. Maisonneuve, *Pattern Recognition* 17, n°2, p. 177-187 (1984)
- [8] S. Bouchet, *Segmentation et Quantification d’images tridimensionnelles*, Paris School of Mines Publication, Internship report, 1999
- [9] J.A. Elliott, A.H. Windle, J.R. Hobdell, G. Eeckhaut, R.J. Oldman, W. Ludwig, E. Boller, P. Cloetens, J. Baruchel, *Journal of Materials Science* 37, p. 1-9 (2002)